Journal of Alloys and Compounds 509 (2011) 669–674

Contents lists available at ScienceDirect

Journal of Alloys and Compounds

journal homepage: www.elsevier.com/locate/jallcom

Review

Crystal structure of the mirror symmetry 10H-type long-period stacking order phase in Mg–Y–Zn alloy

Jian-Xiong Yi[a,b], Bi-Yu Tang[a,b,c,*], Ping Chen[a,b], Dong-Lin Li[a,b], Li-Ming Peng[d], Wen-Jiang Ding[d]

[a] Department of Physics, Xiangtan University, Hunan Province 411105, China
[b] Key Laboratory of Low Dimensional Materials and Application Technology, Ministry of Education (Xiangtan University), Hunan Province 411105, China
[c] School of Chemistry and Chemical Engineering, Guangxi University, Nanning 530004, China
[d] Light Alloy Net Forming National Engineering Research Center, School of Materials Science and Engineering, Shanghai Jiaotong University, Shanghai 200030, China

ARTICLE INFO

Article history:
Received 19 January 2010
Received in revised form 6 September 2010
Accepted 8 September 2010
Available online 20 October 2010

Keywords:
10H-type LPSO phase
Mirror symmetry
Crystal structure
Electronic structure
First-principle electron theory

ABSTRACT

The crystal structure of the 10H-type long-period stacking order structure in Mg–Y–Zn alloy was investigated by first-principle calculations. The calculated results show that the accurate positions and distinctive arrangement of Zn and Y atoms in the most stable 10H-type LPSO phase exhibit mirror symmetry with respect to the atomic layer C_6, which agrees well with the experimental observations. Theoretical calculations still indicate that the mirror symmetry 10H-type ABACBCBCAB phase is not distorted, the lattice distortion of other LPSO phases may originate from the asymmetry of Zn element in the chemical order and stacking order. The obtained electronic density of states (DOS) reveals the underlying mechanism for mirror symmetry of 10H-LPSO phase.

Contents

1. Introduction

As structural materials, Mg alloys have advantages such as low density, good stiffness and the highest strength-to-weight-ratio [1–3]. Especially, because of their ease of recycling the Mg alloys widely used can contribute for maintenance of a clean environment [4]. Up to now, Mg alloys are becoming more and more attractive due to its applications in the microelectronics, automobile and aerospace industries [5–8]. However, the applications of Mg alloys in various fields are still restrained by low tensile strength and inferior ductility.

It is well known that the addition of rare-earth elements and transition metals is one of the most effective methods to optimize the microstructure and improve mechanical properties [9,10]. In recent years, Mg–Y–Zn alloys have received considerable attention due to their excellent mechanical properties and unique microstructures [11–20]. In particular, various novel lamellar structure of long-period stacking order (LPSO) phases have been observed, including 6H, 10H, 14H, 18R and 24R [21–31]. The 6H and 14H structure are commonly observed in conventional casting production [22], while 18R is the main phase by rapid solidification (RS) processing [23]. According to structural feature revealed by electron diffraction experiments, CTEM and HRTEM observa-

---

* Corresponding author at: Department of Physics, Xiangtan University, Hunan Province 411105, China. Tel.: +86 732 8292195; fax: +86 732 8292468.
E-mail address: tangbiyu@xtu.edu.cn (B.-Y. Tang).

0925-8388/$ – see front matter © 2010 Elsevier B.V. All rights reserved.
doi:10.1016/j.jallcom.2010.09.140

tions, 10H phase has mirror symmetry with ABACBCBCAB stacking sequence [21]. Naturally, the special mirror symmetry of stacking sequence would be related to the distinctive atomic configuration especially the distribution of Zn and Y in the novel structure, and further show novel mechanical properties. So the 10H-LPSO structure with the perfect mirror symmetry stacking sequence would be very interesting, and should be given considerable attention.

Unfortunately, 10H LPSO is less commonly observed, and has been less investigated experimentally, so the atomic arrangement rule of Y and Zn elements in the mirror symmetry stacking sequence is still not well understood. In order to get a deeper insight into the detailed atomic configurations and the arrangement role of the Y and Zn in the structural evolution, theoretical investigation is necessary. In this paper, we have carried out first-principles calculations for the 10H LPSO structure in Mg–Y–Zn alloys based the density functional theory within the generalized gradient approximation (GGA). In the present work, the mirror symmetry stacking sequence and chemical order of Zn and Y element in 10H LPSO phase were determined theoretically for the first time, the geometrical evolution and the lattice distortion were also investigated in detail, and the electronic structures were further discussed.

2. Computational details

The present calculations were performed using the Vienna ab initio Simulation Package [32] based on density functional theory (DFT). The well established Predew-Wang (PW91) version of the generalized gradient approximation (GGA) was used to describe the exchange-correlation functional [33], and the valence electron–core interaction was described by PAW potentials [34] with Mg ($2p^6 3s^2$), Y ($4p^6 4s^2 4d^1 5s^2$) and Zn ($3d^{10} 4s^2$) as valence states. To ensure enough convergence, the plane-wave energy cutoff was chosen to be 350 eV, and the Brillouin zone was sampled with a mesh of $5 \times 5 \times 2$ generated by Monkhorst-Pack method [35]. The structural optimization was performed via the conjugate gradient method by full relaxation of the shape and volume of unit cell as well as internal coordinates of atoms, until the forces on atoms is converged to less than 0.01 eV/Å. Then the calculations of total energy and density of states were performed using the linear tetrahedron method with Blöchl correction [36].

3. Results and discussion

3.1. Crystal structure of mirror symmetry stacking

Because LPSO phase is not only stacking ordered but also chemically ordered structure [22], the crystal structure of LPSO phase is sensitive to the Zn and Y concentrations, different contents of Zn and Y would lead to adjustment of the crystal structure. On the other hand, it was also indicated by experiments that the ratio of Y/Zn in LPSO phase was approximately between 1 and 3 [37–39]. Up to now, the chemical compositions of $Mg_{97}Zn_1Y_2$, $Mg_{94}Zn_2Y_4$, $Mg_{91}Zn_3Y_6$, $Mg_{87}Zn_3Y_{10}$, $Mg_{90}Zn_4Y_6$, $Mg_{88}Zn_4Y_8$ (at.%) have been found in the five kinds of LPSO structures, respectively [40,41]. To investigate the mirror symmetry of 10H LPSO structures in Mg–Y–Zn alloy, the various chemical compositions must be determined theoretically. For the sake of convenient description, 10H-type ABACBCBCAB LPSO structure was marked as $A_1B_2A_3C_4B_5C_6B_7C_8A_9B_{10}$ in the present study and the subscript of ten numbers are used to distinguish the different atomic layers. Here, a unit cell of $3 \times 3 \times 5$ (10 layers) was used, which contains 90 atoms. Fig. 1 shows a 3×3 unit cell in the atomic plane of the 10H-LPSO phase perpendicular to c-axis with yellow, gray and green circles representing atoms in the A, B and C layer, respectively.

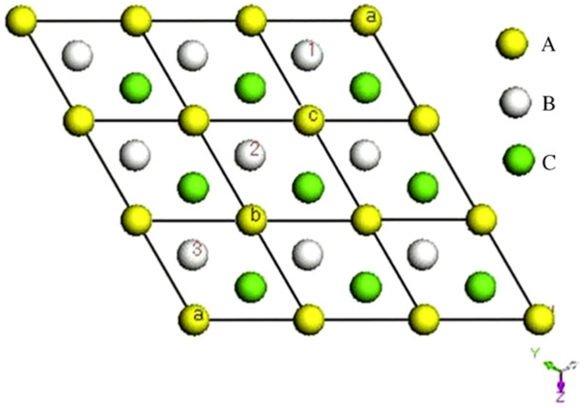

Fig. 1. The 3×3 unit cell in the basal plane of structural model for 10H-LPSO phase, in which yellow, gray and green circles represent the A, B and C layer atoms, respectively. (For interpretation of the references to color in this figure legend, the reader is referred to the web version of the article.)

The calculated results in Table 1 show that when the additive atom is only one Zn or Y atom, the total energy for the additive atom in the symmetry layers which respect to the atomic layer C_6 are equal. For example, $E_{B_2} = E_{B_{10}}$, $E_{A_3} = E_{A_9}$, and so on. Therefore, when the 10H-LPSO phase contains only one Y or Zn atom, the arrangement and distribution of Y or Zn atom in the 10H LPSO phase exhibit always mirror symmetry. Furthermore, when Y or Zn atom is located in the A_1, B_2, C_6 and B_{10} layers the total energy is relatively lower. Fig. 2 visually shows the mirror symmetry of the total energies for Zn atom in different layers of 10H-LPSO structure. Consequently, the Zn atom would be located in B_2 or B_{10} layer, and the Y atom would be located in A_1 layer due to the lowest energy.

As one Zn atom and one Y atom are added simultaneously, there are two ways of addition of the substitution atoms. One way is that Zn atom firstly occupied in B_{10} layer and kept it unchanged, and then the Y atom was added in different layers. Similarly, the other way is Y atom occupied firstly in the A_1 layer, and then the Zn atom was added. The calculation results in Tables 2–4 shows that when Zn and Y atoms are located simultaneously on A_1 layer, the total energy was the lowest. Furthermore, Y atom firstly located at position a in A_1 layer in Fig. 1, then Zn atom located at position b in the vicinity position of Y atom. It is noted that given the small difference in energy between different variants, Zn atoms may not only occupy the B_2 and B_{10} layers, but also A_1 or C_6, Y as well B_2 or C_6. However, it such an arrangement also does not change the symmetric feature. From the thermodynamic point of view, the partial enthalpy for ZnY is −151 kJ/mol, which is a far higher negative value than −27 kJ/mol for ZnMg, so Zn is more likely to form bonding with Y than Mg [42]. The calculated result is consistent with the experimental observations.

When two Zn or Y atoms are added, the calculation results in Table 5 indicate that the two of substitution atoms were not limited in the single layer, but diffused into two different atoms layers B_2 and B_{10}, being symmetrical with respect to the atomic layer C_6. Therefore, the 10H-LPSO structure of $Mg_{88}Zn_2$ and $Mg_{88}Y_2$ alloys also exhibit strict mirror symmetry with respect to the atomic layer C_6.

When a higher ratio of substitution atoms x at.%Zn + y at.%Y was added into 10H-LPSO structure, following the above procedure in which Zn and/or Y atom was added eventually one by one, the accurate positions and arrangement rule of substituted atoms were determined completely. By a large number of calculations, the accu-

Table 1
The total energies with the 1Zn or 1Y substituted atoms, "Δ" represent the 1Zn or 1Y substituted atoms, (–) means no atom added.

Layer	A_1	B_2	A_3	C_4	B_5	C_6	B_7	C_8	A_9	B_{10}	Total energy for 1Zn (eV)	Total energy for 1Y (eV)
1	Δ	–	–	–	–	–	–	–	–	–	−136.0917	−141.6786
2	–	Δ	–	–	–	–	–	–	–	–	−136.0921	−141.6786
3	–	–	Δ	–	–	–	–	–	–	–	−136.0871	−141.4861
4	–	–	–	Δ	–	–	–	–	–	–	−136.0870	−141.4940
5	–	–	–	–	Δ	–	–	–	–	–	−136.0759	−141.4940
6	–	–	–	–	–	Δ	–	–	–	–	−136.0917	−141.6785
7	–	–	–	–	–	–	Δ	–	–	–	−136.0759	−141.4940
8	–	–	–	–	–	–	–	Δ	–	–	−136.0870	−141.4940
9	–	–	–	–	–	–	–	–	Δ	–	−136.0871	−141.4861
10	–	–	–	–	–	–	–	–	–	Δ	−136.0921	−141.6786

Table 2
The total energies with the 1Zn + 1Y substituted atoms, Zn atom firstly occupied in B_{10} layer and kept it unchanged, (–) means no atom added.

Layer	A_1	B_2	A_3	C_4	B_5	C_6	B_7	C_8	A_9	B_{10}	Total energy (eV)
1	1Y	–	–	–	–	–	–	–	–	1Zn	−141.3254
2	–	1Y	–	–	–	–	–	–	–	1Zn	−141.3151
3	–	–	1Y	–	–	–	–	–	–	1Zn	−141.1822
4	–	–	–	1Y	–	–	–	–	–	1Zn	−141.1234
5	–	–	–	–	1Y	–	–	–	–	1Zn	−141.1340
6	–	–	–	–	–	1Y	–	–	–	1Zn	−141.3129
7	–	–	–	–	–	–	1Y	–	–	1Zn	−141.1066
8	–	–	–	–	–	–	–	1Y	–	1Zn	−141.2029
9	–	–	–	–	–	–	–	–	1Y	1Zn	−141.2945
10	–	–	–	–	–	–	–	–	–	1Zn + 1Y	−141.3550

Table 3
The total energies with the 1Zn + 1Y substituted atoms, Y atom firstly occupied in A_1 layer and kept it unchanged, (–) means no atom added.

Layer	A_1	B_2	A_3	C_4	B_5	C_6	B_7	C_8	A_9	B_{10}	Total energy (eV)
1	1Zn + 1Y	–	–	–	–	–	–	–	–	–	−141.3563
2	1Y	1Zn	–	–	–	–	–	–	–	–	−141.3189
3	1Y	–	1Zn	–	–	–	–	–	–	–	−141.3131
4	1Y	–	–	1Zn	–	–	–	–	–	–	−141.1124
5	1Y	–	–	–	1Zn	–	–	–	–	–	−141.2946
6	1Y	–	–	–	–	1Zn	–	–	–	–	−141.3002
7	1Y	–	–	–	–	–	1Zn	–	–	–	−141.3084
8	1Y	–	–	–	–	–	–	1Zn	–	–	−141.3152
9	1Y	–	–	–	–	–	–	–	1Zn	–	−141.3007
10	1Y	–	–	–	–	–	–	–	–	1Zn	−141.3254

rate positions of substituted atoms of the most stable 10H-LPSO phases were shown in Table 6. Clearly, with increasing of substitution atoms, when Zn or Y atoms were even numbers, one half of Zn or Y is located in the B_2 layer, the other half locates in the B_{10} layer. If Zn or Y atoms were odd numbers, one Zn or one Y atom would be located in the A_1 layer. The remainder would arrange as the case for both of Zn and Y atoms being even numbers. Excitingly, the mirror symmetry of substitution atoms in 10H-LPSO phases is always remained.

In terms of the present calculations, each layer could be substituted at most by 3 Y and/or Zn atoms. If Y and Zn atoms were further added, the further added Y and Zn atoms would be located in the C_6 stacking layer on the basis of the energy minimum principle. Therefore, with the increasing of the substitution atoms, the arrangement of Zn and Y atom always remain the mirror symmetry respect to the C_6 atomic layer plane. Experiments showed that most Zn and Y atoms are located in stacking fault layers at the two ends of the LPSO phase, a small amount of additives are distributed in the interior of LPSO phase [41]. The present investigation is in good agreement with the experimental observation. Based on the distribution of the Zn and Y atoms in the C_6 stacking layers, it is interested to note that the six layer building block "$A_1B_2A_3C_4B_5C_6$" possesses an atomic arrangement similar to the 6H-LPSO structure. Therefore, the present investigation implies tendency and characteristics of inter-transformation between 10H-and 6H-type LPSO phases. It is crucial to further reveal the inter-transformation of various LPSO phases and the microscopic rule. Relevant study is under the way. It is noteworthy that all calculation are done assuming $T = 0$ K. However, at room or even higher temperature,

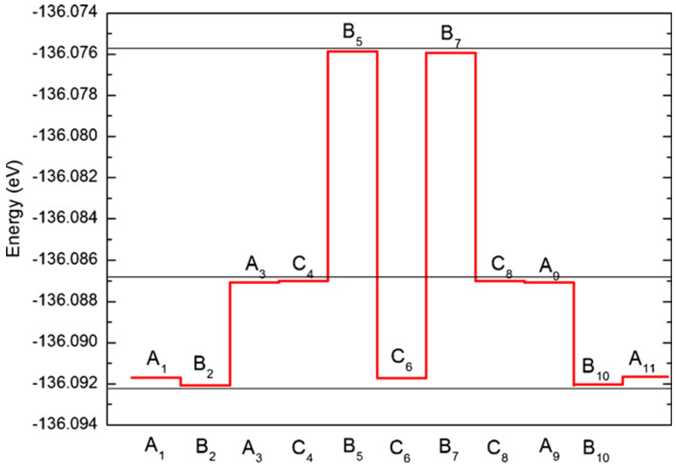

Fig. 2. The mirror symmetry of total energy with respect to atomic layer C_6 for Zn atom in different layers of 10H-LPSO structure.

Table 4
The total energies with the 1Zn +1Y substituted atoms which added in the same layer simultaneously, "Δ" represent the 1Zn + 1Y substituted atoms, (–) means no atom added.

Layer	A_1	B_2	A_3	C_4	B_5	C_6	B_7	C_8	A_9	B_{10}	Total energy (eV)
1	–	Δ	–	–	–	–	–	–	–	–	−141.3550
2	–	–	Δ	–	–	–	–	–	–	–	−141.3224
3	–	–	–	Δ	–	–	–	–	–	–	−141.2965
4	–	–	–	–	Δ	–	–	–	–	–	−141.3057
5	–	–	–	–	–	Δ	–	–	–	–	−141.3250
6	–	–	–	–	–	–	Δ	–	–	–	−141.3057
7	–	–	–	–	–	–	–	Δ	–	–	−141.2965
8	–	–	–	–	–	–	–	–	Δ	–	−141.3224
9	–	–	–	–	–	–	–	–	–	Δ	−141.3550

Table 5
The total energies with the 2Zn or 2Y substituted atoms, (–) means no atom added.

Layer	A_1	B_2	A_3	C_4	B_5	C_6	B_7	C_8	A_9	B_{10}	Total energy (eV)
1	–	1Zn	–	–	–	–	–	–	–	1Zn	−135.7162
2	1Zn	–	–	–	–	–	–	–	–	1Zn	−135.7121
3	1Zn	1Zn	–	–	–	–	–	–	–	–	−135.7057
4	–	2Zn	–	–	–	–	–	–	–	–	−135.6853
5	–	1Zn	–	–	–	–	–	1Zn	–	–	−135.6985
6	–	1Y	–	–	–	–	–	–	–	1Y	−146.8010
7	1Y	–	–	–	–	–	–	–	–	1Y	−146.7929
8	–	–	1Y	1Y	–	–	–	–	–	–	−146.5538
9	–	2Y	–	–	–	–	–	–	–	–	−146.5427
10	–	1Y	–	–	–	1Y	–	–	–	–	−146.6336

Table 6
The best optimized and accurate positions of substituted atoms of 10H LPSO phases with the xY + yZn ($x+y\geq 3,\ 1<x\leq 4,\ 1<y\leq 8$) substituted atoms, (–) means no atom added.

xY + yZn	A_1	B_2	A_3	C_4	B_5	C_6	B_7	C_8	A_9	B_{10}
1Zn + 2Y	1Zn	1Y	–	–	–	–	–	–	–	1Y
1Zn + 3Y	1Zn + 1Y	1Y	–	–	–	–	–	–	–	1Y
2Zn + 1Y	1Y	1Zn	–	–	–	–	–	–	–	1Zn
2Zn + 2Y	–	1Zn + 1Y	–	–	–	–	–	–	–	1Zn + 1Y
2Zn + 3Y	1Y	1Zn + 1Y	–	–	–	–	–	–	–	1Zn + 1Y
2Zn + 4Y	–	1Zn + 2Y	–	–	–	–	–	–	–	1Zn + 2Y
2Zn + 5Y	1Y	1Zn + 2Y	–	–	–	–	–	–	–	1Zn + 2Y
2Zn + 6Y	1Y	1Zn + 2Y	–	–	–	1Y	–	–	–	1Zn + 2Y
3Zn + 6Y	1Zn + 1Y	1Zn + 2Y	–	–	–	1Y	–	–	–	1Zn + 2Y
4Zn + 6Y	1Zn + 1Y	1Zn + 2Y	–	–	–	1Zn + 1Y	–	–	–	1Zn + 2Y
4Zn + 7Y	1Zn + 1Y	1Zn + 2Y	–	–	–	1Zn + 2Y	–	–	–	1Zn + 2Y
4Zn + 8Y	1Zn + 2Y	1Zn + 2Y	–	–	–	1Zn + 2Y	–	–	–	1Zn + 2Y

Table 7
The variation of the angle θ (°) between the a^*- and c^*-axes with the concentration and position of Zn and Y elements.

xY + yZn	A_1	B_2	A_3	C_4	B_5	C_6	B_7	C_8	A_9	B_{10}	θ ($a^*\wedge c^*$)
1Zn	–	1Zn	–	–	–	–	–	–	–	–	90°
2Zn	–	1Zn	–	–	–	–	–	–	–	1Zn	90°
2Zn	–	2Zn	–	–	–	–	–	–	–	–	90°
2Zn	1Zn	–	–	–	–	–	–	–	–	1Zn	89.77°
1Zn + 1Y	1Zn + 1Y	–	–	–	–	–	–	–	–	–	90°
1Zn + 2Y	1Zn	1Y	–	–	–	–	–	–	–	1Y	90°
1Zn + 3Y	1Zn + 1Y	1Y	–	–	–	–	–	–	–	1Y	90°
2Zn + 1Y	1Y	1Zn	–	–	–	–	–	–	–	1Zn	90°
2Zn + 1Y	1Zn + 1Y	–	–	–	–	–	–	–	–	1Zn	89.80°
2Zn + 2Y	–	1Zn + 1Y	–	–	–	–	–	–	–	1Zn + 1Y	90°
2Zn + 3Y	1Y	1Zn + 1Y	–	–	–	–	–	–	–	1Zn + 1Y	90°
2Zn + 3Y	1Zn + 2Y	–	–	–	–	–	–	–	–	1Zn + 1Y	89.84°
2Zn + 4Y	–	1Zn + 2Y	–	–	–	–	–	–	–	1Zn + 2Y	90°
2Zn + 5Y	1Y	1Zn + 2Y	–	–	–	–	–	–	–	1Zn + 2Y	90°
2Zn + 6Y	1Y	1Zn + 2Y	–	–	–	1Y	–	–	–	1Zn + 2Y	90°
3Zn + 6Y	1Zn + 1Y	1Zn + 2Y	–	–	–	1Y	–	–	–	1Zn + 2Y	90°
4Zn + 6Y	1Zn + 1Y	1Zn + 2Y	–	–	–	1Zn + 1Y	–	–	–	1Zn + 2Y	90°
4Zn + 7Y	1Zn + 1Y	1Zn + 2Y	–	–	–	1Zn + 2Y	–	–	–	1Zn + 2Y	90°
4Zn + 8Y	1Zn + 2Y	1Zn + 2Y	–	–	–	1Zn + 2Y	–	–	–	1Zn + 2Y	90°

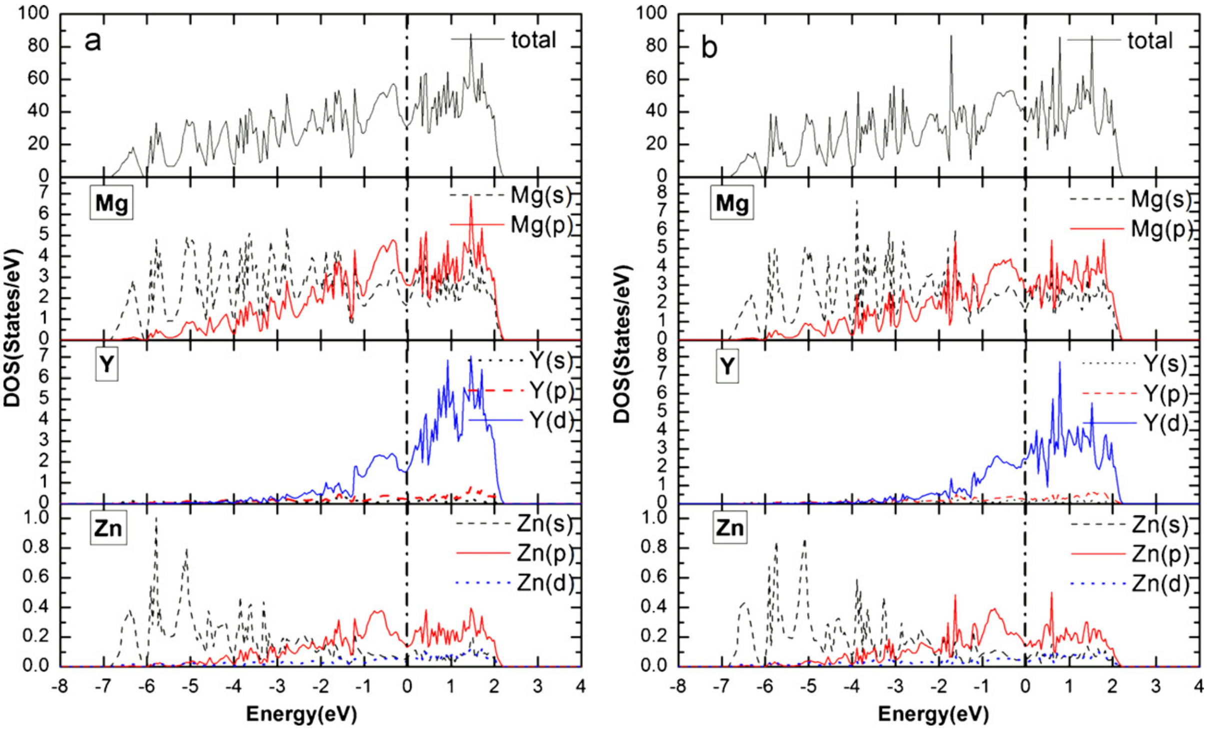

Fig. 3. Total and Partial density of states of 10H-LPSO $Mg_{85}Y_3Zn_2$ without distortion (a) and with lattice distortion (b). The Fermi level is set at zero.

entropy becomes more important. Due to the small energy differences of the substitution models discussed here, incorporation of entropy may lead to disordered structures. So 10H LPSO structure is rarely observed experimentally in comparison with other phases.

3.2. Lattice distortion and electronic structure

Lattice distortion is an important feature of the LPSO structures in Mg–Y–Zn alloy, it means that the *c*-axis is not perpendicular to the *a*-axis, which was observed in 6H and 18R [22,23]. Separation and segregation of Zn and Y atoms are considered to result in the lattice distortion [43]. Our previous work revealed that the Zn atoms dispersed in two different layers are the origin of distortion in 6H-LPSO structure [40]. Although the distortion of 10H-type ABACBCBCAB LPSO structure is not reported in experiments up to now, it is interesting to discuss theoretically this problem for the 10H-type ABACBCBCAB structure with the mirror symmetry. The calculated results of different chemical compositions for 10H-type ABACBCBCAB in Table 7 clearly show no distortion, which is different from the case in 6H LPSO phase, where distortion happened when two Zn atoms occupied in the two fault layers at the two ends. For further investigation, the two Zn atoms in the 10H LPSO phase are also assumed to located in the two fault layers at the two end, then the calculations show that distortion happened, the angle between the *a*-axis and *c*-axis is less than 89.77°. So an asymmetry of the chemical order with respect to the 10H-type stacking order would result in the lattice distortion. It may be further inferred that the lattice distortion in the LPSO phases is likely to originate from the asymmetry arrangement of the Zn element with respect to the central layer of the LPSO structure, which is consistent with the conjecture in Ref. [19]. On the other hand, the further calculations show that the lattice distortion due to the dispersion of Zn atoms in two asymmetry layers can be weaken with incorporation of Y atoms due to the intimate arrangement of Zn and Y atoms in the same layer.

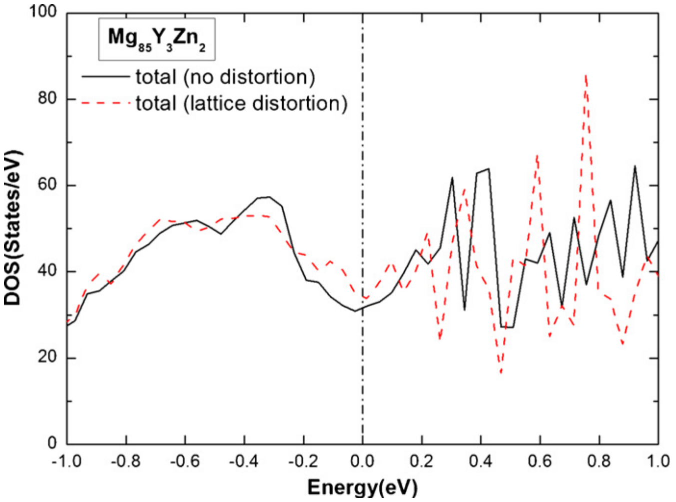

Fig. 4. Total density of states near Fermi energy for the 10H-LPSO $Mg_{85}Y_3Zn_2$ with and without distortion.

Because 10H-type ABACBCBCAB structure shows mirror symmetry without distortion, the proliferation of thermodynamic equilibrium conditions of experimental formation must be required. So 10H-LPSO structure is difficult to be formed. Amiya pointed out that such novel structure could be developed by the control of the atomic scale segregation mode [44].

In order to further study the characteristic of bonding in novel 10H-LPSO structure and the underlying mechanism of mirror symmetry, the electronic density of states (DOS) is calculated. For comparison, we choose the prefect 10H-LPSO $Mg_{85}Y_3Zn_2$ phase without distortion and distorted 10H-LPSO $Mg_{85}Y_3Zn_2$ phase in which one Zn and two Y atoms were located in A_1 layer, the remainder one Y and one Zn were located at B_{10} layer in terms of the general structural model of atom arrangement in the LPSO phases. The corresponding DOS are shown in Fig. 3(a) and (b), respectively. It can be seen that the overall shapes of DOS curves without distortion are similar to that of 10H-LPSO structure with lattice distortion. In the whole region, the calculated total DOS is dominated by the Mg-s states and Mg-p states because of the high content of Mg atom in structure. And the Y-d states and Zn-p states are the significant contribution especially around the Fermi level. Furthermore, the total DOS also show that there are deep valleys close to the Fermi level, the valley pseudogap indicates the presence of covalent bond [45]. In order to reveal the subtle different of the DOS, Fig. 4 shows the total densities of states at Fermi level for 10H-LPSO structure with and without distortion. A closer inspection shows that the electron density-of-states at the Fermi level for the mirror symmetry 10H-LPSO structure without distortion is lower than that of 10H-LPSO structure with lattice distortion, indicating that the hybridization of Zn-p and Mg-p states with Y-d states are stronger for 10H-LPSO structure without distortion, while the hybridization for 10H-LPSO structure with lattice distortion is relatively weaker. It is generally believed that a reduction in DOS at the Fermi level is benefit to the stability of a given structure [46]. That is, the lower is the value, the more is the stability. Moreover, as a conventional consideration, the stronger covalent bond in YZn and YMg clusters for 10H-LPSO structure without distortion may lead to higher yield strength in (Y,Zn)-rich region of the microstructure in alloys. On the contrary, the mechanical properties of the LPSO structure with lattice distortion would be affected due to the weaker covalent bond. So mirror symmetry without distortion is conducive to the stability of 10H-LPSO structure, and further favorable for the mechanical properties of Mg-based alloy.

4. Conclusions

In summary, a first-principles calculation based on density functional theory is used to investigate the crystal structure of the 10H-type LPSO phase. The calculation results showed that most stable positions of all the substitution atoms exhibited mirror symmetry with respect to the plane of C_6 atomic layer. The present theoretical calculations revealed the unique feature of arrangement and distribution of Y and Zn atoms in the mirror symmetry 10H-type LPSO phase. Furthermore, it is found that the most stable 10H-type phase with mirror symmetry has not structural distortion, the lattice distortion in the LPSO phase is likely to originate from the asymmetry arrangement of the Zn element with respect to the central layer of the LPSO structure. The electronic density of states (DOS) indicated that mirror symmetry without distortion is conducive to the stability of 10H-LPSO structure.

Acknowledgments

This work is supported by Natural Science Foundation of China (50861002), of Hunan Province (08JJ6001) and Guangxi Province (0991051), also Key Laboratory of Materials Design and Preparation Technology of Hunan Province (KF0803) and the Scientific Research Foundation of Guangxi University (X071117).

References

[1] C. Potzies, K.U. Kainer, Adv. Eng. Mater. 6 (2004) 281.
[2] K.U. Kainer, Magnesium Alloys and Their Applications, Wiley, New York, 2000.
[3] X. Zhang, D. Kevorkov, M.O. Pekguleryuz, J. Alloys Compd. 501 (2010) 366.
[4] G. Garcés, M. Maeso, I. Todd, P. Pérez, P. Adeva, J. Alloys Compd. 432 (2007) L10.
[5] S.W. Lee, H.Y. Wang, Y.L. Chen, J.W. Yeh, C.F. Yang, Adv. Eng. Mater. 6 (2004) 948.
[6] H. Kohlmann, Y.S. Zhao, M.F. Nicol, J. McClure, Z. Kristallogr. 223 (2008) 706.
[7] Y. Terada, T. Sato, J. Alloys Compd. 504 (2010) 261.
[8] R. Ferragut, F. Moia, F. Fiori, D. Lussana, G. Riontino, J. Alloys Compd. 495 (2010) 408.
[9] E.F. Emley, Principles of Magnesium Technology, Pergamon Press, Oxford, 1966, p. 264.
[10] L.L. Rokhlin, Magnesium Alloys Containing Rare Earth Metals: Structure and Properties, CRC Press, 2003, p.135.
[11] Q.M. Peng, X.L. Hou, L.D. Wang, Mater. Des. 30 (2009) 292.
[12] G. Riontinoa, M. Massazza, D. Lussanaa, Mater. Sci. Eng. A 494 (2008) 445.
[13] M. Nishida, T. Yamamuro, M. Nagano, Y. Morizono, Y. Kawamura, Mater. Sci. Forum 419 (2003) 715.
[14] Y. Kawamura, K. Hayashi, A. Inoue, T. Masumoto, Mater. Trans. 42 (2001) 1172.
[15] Y.M. Zhu, A.J. Morton, J.F. Nie, Acta Mater. 58 (2010) 2936.
[16] M. Yamasaki, Y. Kawamura, Scripta Mater. 60 (2009) 264.
[17] K. Hagihara, N. Yokotani, Y. Umakoshi, Intermetallics 18 (2010) 267.
[18] P. Chen, D.-L. Li, J.-X. Yi, B.-Y. Tang, L.-M. Peng, W.-J. Ding, Alloy Compd. J. 485 (2009) 672.
[19] K. Liu, J.H. Zhang, H.Y. Lu, D.X. Tang, L.L. Rokhlin, F.M. Elkin, J. Meng, Mater. Des. 31 (2010) 210.
[20] K. Hagihara, A. Kinoshita, Y. Sugino, M. Yamasaki, Y. Kawamura, H.Y. Yasuda, Y. Umakoshi, Intermetallics 18 (2010) 1079.
[21] M. Matsuda, S. Ii, Y. Kawamura, Y. Ikuhara, M. Nishida, Mater. Sci. Eng. A 393 (2005) 269.
[22] E. Abe, Y. Kawamura, K. Hayashi, A. Inoue, Acta Mater. 50 (2002) 3845.
[23] M. Matsuda, S. Ii, Y. Kawamura, Y. Ikuhara, M. Nishida, Mater. Sci. Eng. A 386 (2004) 447.
[24] Z.P. Luo, S.Q. Zhang, J. Mater. Sci. Lett. 19 (2000) 813.
[25] M. Yamasaki, T. Anan, S. Yoshimoto, Y. Kawamura, Scripta Mater. 53 (2005) 799.
[26] A. Datta, U. Ramamurty, S. Ranganathan, U.V. Waghmare, Comput. Mater. Sci. 37 (2006) 69.
[27] T. Honma, T. Ohkubo, S. Kamado, K. Hono, Acta Mater. 55 (2007) 4137.
[28] M. Yamasaki, M. Sasaki, M. Nishijima, K. Hiraga, Y. Kawamura, Acta Mater. 55 (2007) 6798.
[29] M. Nishijima, K. Hiraga, M. Yamasaki, Y. Kawamura, Mater. Trans. 49 (2008) 227.
[30] B.S. Wang, Y.B. Liu, J. An, Mater. Trans. 49 (2008) 1768.
[31] Y.J. Wu, X.Q. Zeng, D.L. Lin, L.M. Peng, W.J. Ding, J. Alloys Compd. 477 (2009) 193.
[32] G. Kresse, J. Furthmuller, Phys. Rev. B 54 (1996) 11169.
[33] J.P. Perdew, J.A. Chevary, S.H. Vosko, K.A. Jackson, M.R. Pederson, D.J. Singh, C. Fiolhais, Phys. Rev. B 46 (1992) 6671.
[34] P.E. Blöchl, Phys. Rev. B 50 (1994) 17953.
[35] H.J. Monkhorst, J.D. Pack, Phys. Rev. B 13 (1976) 5188.
[36] P.E. Blöchl, O. Jepsen, O.K. Andersen, Phys. Rev. B 49 (1994) 16223.
[37] D.H. Ping, K. Hono, Y. Kawamura, D.H. Ping, K. Hono, Y. Kawamura, A. Inoue, Philos. Mag. Lett. 82 (2002) 543.
[38] J. Lee, K. Sato, T.J. Konno, K. Hiraga, Mater. Trans. 50 (2009) 222.
[39] S. Yoshimoto, M. Yamasaki, Y. Kawamura, Mater. Trans. 47 (2006) 959.
[40] Y.F. Wang, Z.Z. Wang, N. Yu, X.Q. Zeng, W.J. Ding, B.Y. Tang, Scripta Mater. 58 (2008) 807.
[41] T. Itoi, T. Seimiya, Y. Kawamura, M. Hirohashi, Scripta Mater. 51 (2004) 107.
[42] M. Matsuura, M. Sakurai, K. Amiya, A. Inoue, J. Alloys Compd. 353 (2003) 240.
[43] A. Inoue, M. Matsushita, Y. Kawamura, K. Amiya, K. Hayashi, J. Koike, Mater. Trans. 43 (2002) 580.
[44] K. Amiya, T. Ohsuna, A. Inoue, Mater. Trans. 44 (2003) 2151.
[45] P. Ravindran, L. Fast, P.A. Korzhavyi, B. Johansson, J. Wills, O. Eriksson, J. Appl. Phys. 84 (1998) 4891.
[46] C.L. Fu, X.D. Wang, Y.Y. Ye, K.M. Ho, Intermetallics 7 (1999) 179.